Research in Astron. Astrophys. **2010** Vol. **10** No. **7**, 612–620
http://www.raa-journal.org *http://www.iop.org/journals/raa*

***R**esearch in*
***A**stronomy and*
***A**strophysics*

EDITOR'S RECOMMENDATION

New background quasars in the vicinity of the Andromeda Galaxy discovered with the Guoshoujing Telescope (LAMOST)

Zhi-Ying Huo[1], Xiao-Wei Liu[1,2], Hai-Bo Yuan[1], Hui-Hua Zhang[1], Yong-Heng Zhao[3], Jian-Jun Chen[3], Zhong-Rui Bai[3], Hao-Tong Zhang[3], Hua-Wei Zhang[1], Ruben García-Benito[2], Mao-Sheng Xiang[4], Hong-Liang Yan[3], Juan-Juan Ren[3], Shi-Wei Sun[3], Yong Zhang[5], Ye-Ping Li[5], Qi-Shuai Lu[5], You Wang[5], Ji-Jun Ni[5] and Hai Wang[5]

[1] Department of Astronomy, Peking University, Beijing 100871, China; *x.liu@pku.edu.cn*
[2] Kavli Institute for Astronomy and Astrophysics, Peking University, Beijing 100871, China
[3] National Astronomical Observatories, Chinese Academy of Sciences, Beijing 100012, China
[4] Department of Astronomy, Beijing Normal University, Beijing 100875, China
[5] Nanjing Institute of Astronomical Optics & Technology, Chinese Academy of Sciences, Nanjing 210042, China

Received 2010 April 6; accepted 2010 June 3

Abstract We present preliminary analyses of spectra of quasar candidates in two Guoshoujing Telescope (GSJT, formerly named the Large Sky Area Multi-Object Fiber Spectroscopic Telescope - LAMOST) test fields near M 31 where one is close to the optical center of the disk and the other is towards the northeastern outskirts of the halo, obtained during the early stage of the GSJT commissioning in the last season of 2009. Both fields contain background low-redshift quasar candidates selected from the SDSS photometry. In total, 14 new quasars with redshifts up to 2 and i magnitudes between 16.7 and 19.2, are discovered, including 7 within the 2.5° central region of M 31. We briefly discuss the potential applications of these newly discovered bright quasars.

Key words: galaxies: individual (M31) — quasars: general — quasars: emission lines

1 INTRODUCTION

Quasars are the most luminous and energetic objects in the universe. They have long been used to study a variety of astrophysical problems, such as the reionization (e.g. Haiman & Loeb 1999) and large scale structure (e.g. Boyle et al. 2000) of the universe, properties of the intergalactic medium (e.g. Murdoch et al. 1986), the formation and evolution of galaxies (e.g. Gebhardt et al. 2000) and central supermassive black holes (e.g. Corbett et al. 2003).

Low redshift quasars behind nearby galaxies are particularly interesting. Observations of absorption line systems in their spectra allow one to probe the distribution and chemical composition of the interstellar and intracluster medium and to study the rotation curves well beyond the optical radii (e.g. Bowen et al. 1995). They can also serve as references to determine the proper motions of nearby galaxies (e.g. Anguita et al. 2000). In a series of papers, Pocock et al. (1984), Monk et al. (1986) and Monk et al. (1988) presented results of their long-term campaign to search for quasars and other objects behind nearby galaxies. Tinney et al. (1997) and Tinney (1999) obtained a sample of quasars behind the southern satellite galaxies of the Milky Way, with the purpose of studying their proper motions. Geha et al. (2003) identified 47 quasars behind the Magellanic Clouds from their photometric variabilities using the MACHO database. Dobrzycki et al. (2002, 2003) also discovered several quasars behind the Magellanic Clouds. For the Andromeda Galaxy M 31, Crampton et al. (1997) presented several quasar candidates. More recently, SDSS (Sloan Digital Sky Survey; York et al. 2000) obtained three spectroscopic plates in two fields in the outer halo of M 31, targeting low-redshift quasars (c.f. Adelman-McCarthy et al. 2006, 2007). The data have not yet been published as far as we are aware of. We examined the SDSS dataset and found that in total 145 quasar candidates were targeted, with 75 of them spectroscopically confirmed.

The GSJT is a newly built quasi-meridian reflecting Schmidt telescope (Wang et al. 1996; Su et al. 1998; Xing et al. 1998; Zhao 2000; Cui et al. 2004; Zhu et al. 2006; Cui et al. in preparation; c.f. *http://www.lamost.org/website/en/*), located in Xinglong Station of National Astronomical Observatories, Chinese Academy of Sciences, 114 km northeast of Beijing. It has an effective aperture of about 4 m and a field of view (FoV) of 5° in diameter. With a parallel fully controllable fiber positioning system, GSJT can simultaneously record spectra of up to 4 000 celestial objects. GSJT is currently undergoing commissioning for technical fine-tuning, performance characterization and optimization, and scientific capability demonstration. For this purpose, a number of test fields have been selected. These fields normally encompass several SDSS spectroscopic plates to facilitate easy comparison of GSJT and SDSS data.

Being the most important member of the Local Group and the nearest archetypical spiral galaxy, M 31 has a large optical radius $R_{25} = 1.5^\circ$ (de Vaucouleurs et al. 1991), which is well matched to the FoV of GSJT, making it a perfect target for GSJT. We have therefore selected two commissioning fields around M 31, one centered on $\mathrm{RA} = 00^{\mathrm{h}}44^{\mathrm{m}}37\overset{\mathrm{s}}{.}2$, $\mathrm{Dec.} = +40^\circ40'45''$ (for simplification, hereafter named as F03), close to its optical nucleus at $\mathrm{RA} = 00^{\mathrm{h}}42^{\mathrm{m}}44\overset{\mathrm{s}}{.}4$, $\mathrm{Dec.} = +41^\circ16'08''$ (de Vaucouleurs et al. 1991), and the other towards the northeastern halo, centered on $\mathrm{RA} = 01^{\mathrm{h}}12^{\mathrm{m}}34\overset{\mathrm{s}}{.}1$, $\mathrm{Dec.} = +45^\circ20'15''$ (hereafter named as F02). A variety of targets were selected for fields F02 and F03, including planetary nebulae (PNe) and candidates (c.f. the accompanying paper by Yuan et al. reporting new PNe discovered in M 31), normal and luminous red galaxies as well as low-redshift quasars and candidates. These were supplemented by stars selected from the point source catalogs of the Two Micron All Sky Survey (2MASS; Skrutskie et al. 2006). Standard stars (F subdwarfs) were selected from the SDSS photometry. About 5 percent of the 4 000 fibers were allocated to measure the sky background. Test observations of F02 and F03 were obtained in the last quarter of 2009. In this paper, we report newly discovered quasars from these early commissioning data.

2 CANDIDATE SELECTION, OBSERVATIONS AND DATA REDUCTION

SDSS scanned two stripes with a total area of 100 square degrees, 5° wide and 20° long, that passed through the central region and southeastern halo of M 31 from northeast to southwest (Adelman-McCarthy et al. 2006, 2007). Quasar candidates were identified as outliers of stellar loci on the SDSS color-color diagrams. Following Richards et al. (2002), we have adopted the following criteria for selecting low-redshift quasar candidates:

$$14.0 < i_{\mathrm{psf}} < 19.1, \qquad (1)$$

$$r_{\mathrm{psf}} - r_{\mathrm{petro}} \leq 0.24, \qquad (2)$$

$$-0.27 \leq u - g < 0.71, \quad (3)$$
$$-0.24 \leq g - r < 0.35, \quad (4)$$
$$-0.27 \leq r - i < 0.57, \quad (5)$$
$$-0.35 \leq i - z < 0.70. \quad (6)$$

Objects with problematic SDSS PHOTO flags have been excluded. We adopt point-spread function (PSF) magnitudes and correct for the foreground Galactic extinction using the extinction map of Schlegel et al. (1998). To safeguard data quality, we reject objects with PSF magnitude errors exceeding 0.05, 0.025, 0.025, 0.025 and 0.05 mag in u, g, r, i and z, respectively. Figure 1 shows the color-color diagrams of stars and quasar candidates from the SDSS M 31 stripes. Stars and quasar candidates are well separated in the $g - r$ versus $u - g$ diagram. In total, 497 quasar candidates have been selected.

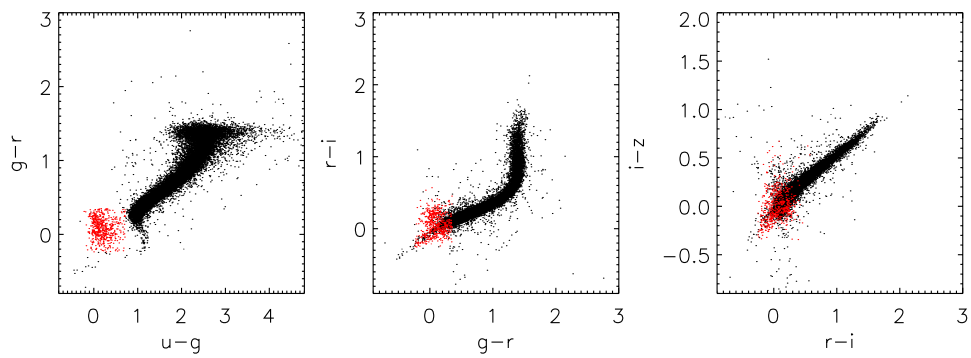

Fig. 1 Color-color diagrams of point sources from the SDSS M 31 stripes. Black dots are stars with magnitudes $16 < i_{\rm psf} < 19.1$, while red dots denote low-redshift quasar candidates. For clarity, only 30 000 stars, randomly selected from a total of 332 860 stars in the field, are shown.

Observations of field F03 close to the M 31 nucleus were obtained on 2009 October 19 and December 15. The outskirt field F02 was observed on 2009 October 20 and December 17. The blue and red arms of each of the 16 spectrographs yield spectra covering wavelength ranges 370–590 nm and 570–900 nm, respectively. Observations in October were obtained without slit masks, yielding a spectral resolving power of $R \sim 1\,000$. In December, slit masks of width half the fiber diameter (3.3′′) were employed, doubling the resolving power to 2 000 at the cost of losing 39 per cent of the incoming light. Additional observations of fields F02 and F03 were obtained in 2009 October and November. They were, however, either obtained under poor observing conditions or with short exposure times, and were therefore not included in the current analysis. In total, 117 low-redshift quasar candidates were targeted, many of them repeatedly in October and December.

The spectra were reduced using the GSJT 2D pipeline (Luo et al. 2004), which is still in an early stage of development. One-dimensional spectra from individual fibers were traced and extracted, then corrected for variations in relative throughputs and spectral responses using flat-field exposures of tungsten lamps. The spectra were then wavelength-calibrated using exposures of arc lamps. Sky spectra measured by sky fibers were then subtracted from source spectra. Analyses of sky emission lines as well as unresolved nebular emission lines of PNe in M 31 yield a resolving power of 1 250 for both blue and red arms for spectra obtained in 2009 October without slit masks. For observations taken in 2009 December with slit masks, an average resolving power of 2 300 and 2 000 is deduced

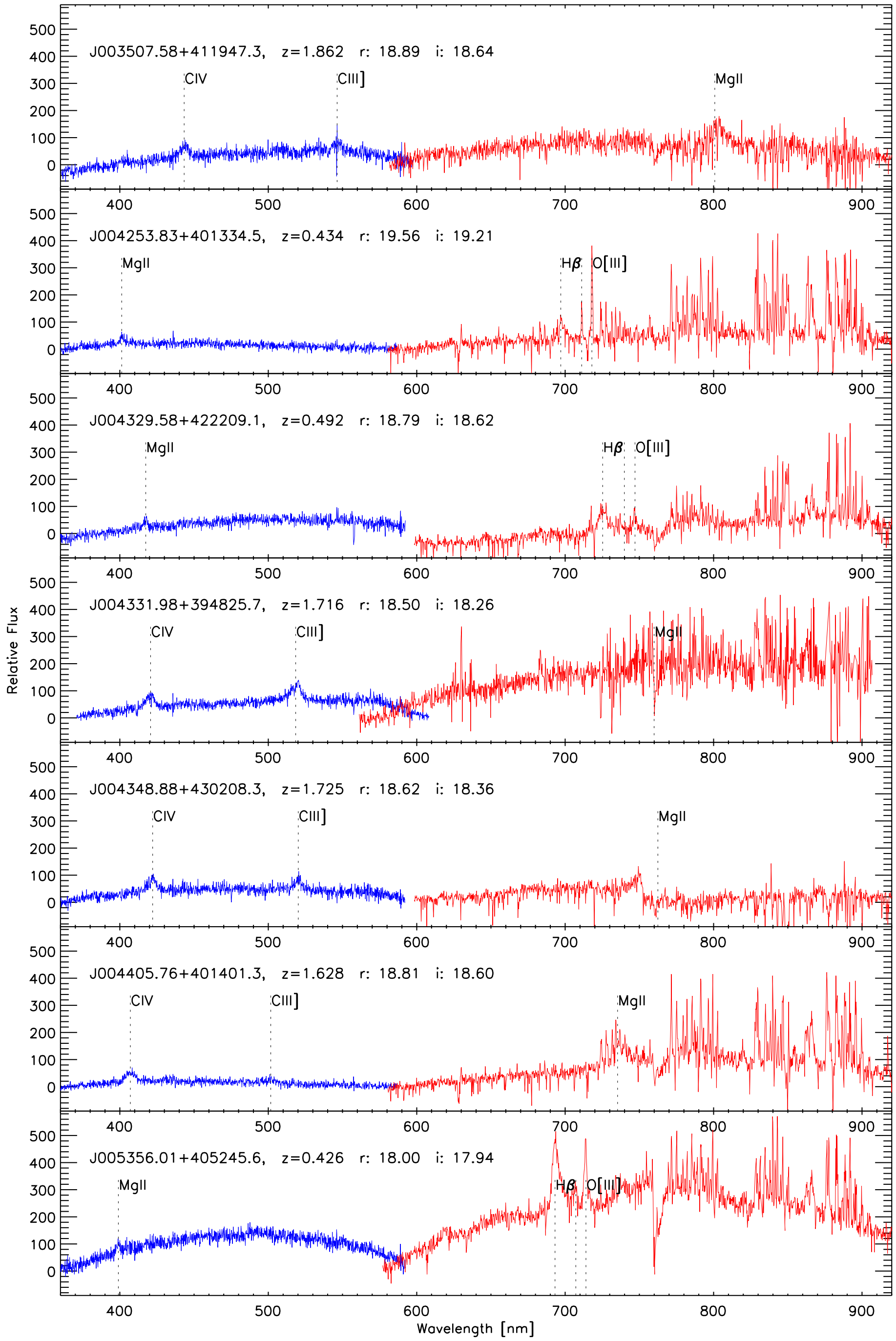

Fig. 2 GSJT spectra of newly discovered quasars, with identified lines labeled. The relative fluxes are in units of counts per pixel.

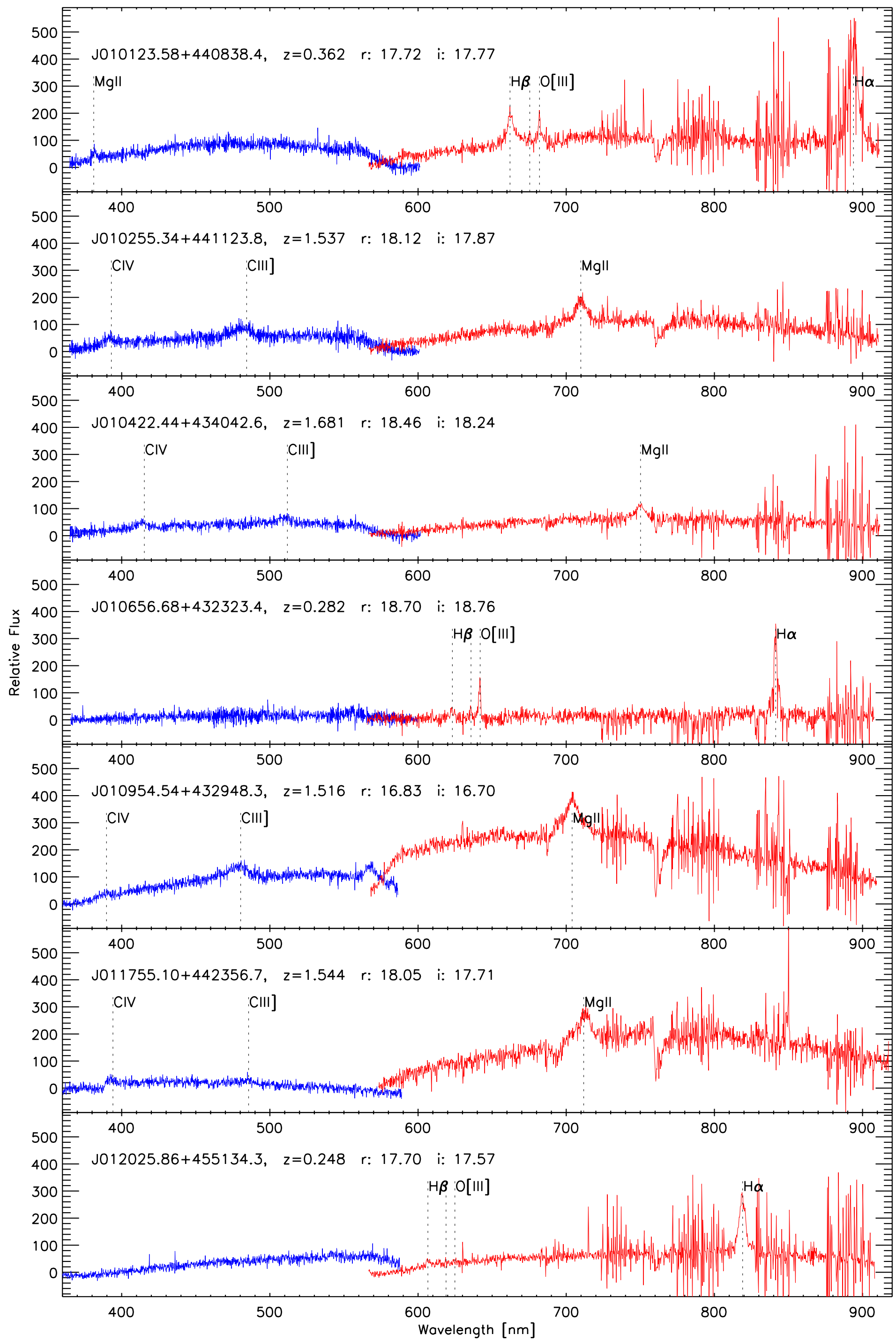

Fig. 2 *Continued.*

Table 1 New Quasars Discovered by GSJT in Commissioning Fields F02 and F03 Near M 31

Object	RA	Dec. (J2000)	SDSS $ugriz$ Magnitudes					A(i)	Obs. date	Fiber ID	z	Notes
J003507.58+411947.3	08.781602	41.329804	18.87	18.86	18.89	18.64	18.58	0.12	2009/10/19	14–09–02	1.862	
J004253.83+401334.5	10.724277	40.226262	19.70	19.44	19.56	19.21	18.81	0.17	2009/10/19	04–06–07	0.434	a
J004329.58+422209.1	10.873266	42.369182	18.96	18.72	18.79	18.62	18.59	0.18	2009/10/19	11–04–22	0.492	b
J004331.98+394825.7	10.883255	39.807151	18.71	18.56	18.50	18.26	18.16	0.12	2009/12/15	05–07–14	1.716	
J004348.88+430208.3	10.953687	43.035645	18.91	18.74	18.62	18.36	18.24	0.17	2009/10/19	11–06–06	1.725	
J004405.76+401401.3	11.023997	40.233708	19.10	18.91	18.81	18.60	18.52	0.15	2009/10/19	04–06–21	1.628	
J005356.01+405245.6	13.483376	40.879324	18.47	18.15	18.00	17.94	17.80	0.12	2009/10/19	13–04–02	0.426	
J010123.58+440838.4	15.348267	44.144009	18.01	17.81	17.72	17.77	17.37	0.18	2009/12/17	02–07–13	0.362	
J010255.34+441123.8	15.730592	44.189945	18.55	18.28	18.12	17.87	18.02	0.16	2009/12/17	02–08–06	1.537	
J010422.44+434042.6	16.093499	43.678496	18.82	18.59	18.46	18.24	18.19	0.15	2009/12/17	02–06–13	1.681	
J010656.68+432323.4	16.736175	43.389832	19.33	19.01	18.70	18.76	18.36	0.16	2009/12/17	02–01–17	0.282	
J010954.54+432948.3	17.477254	43.496741	17.30	17.04	16.83	16.70	16.82	0.15	2009/12/17	01–03–12	1.516	
J011755.10+442356.7	19.479602	44.399093	18.93	18.16	18.05	17.71	17.66	0.15	2009/10/20	08–05–15	1.544	
J012025.86+455134.3	20.107754	45.859526	17.78	17.81	17.70	17.57	17.54	0.15	2009/12/17	13–10–17	0.248	

a: At a distance of 16.22″ from the X-ray source RX J0042.8+4013 (Supper et al. 1997);
b: At a distance of 13.45″ from the X-ray source RX J0043.4+4222 (Supper et al. 2001).

for blue and red arm spectra, respectively. These results are largely in agreement with our expectations. Similarly, analyses of sky emission lines show that the wavelength calibration is accurate to $8\,\mathrm{km\,s^{-1}}$. This is corroborated by a comparison of the measured radial velocities of PNe in M 31 with those in the literature (c.f. Yuan et al. this volume). For the current analysis, no flux-calibration was attempted, even though standard stars were observed. Considering the large uncertainties in the current pipeline processing, in particular in flat-fielding and sky-subtraction, for the moment, the SDSS photometric magnitudes serve as much better measurements of the brightness of our targets.

3 RESULTS AND DISCUSSION

Given that the whole telescope and instrument system are still in the early commissioning stage and their performance is far from optimized, the data presented are unavoidably plagued by various defects. Apart from the overall lower-than-design throughput caused by uncertainties in fiber positioning and large dome seeing, the existence of strong electromagnetic interference patterns in some CCD frames and the very high dark current levels of some CCDs, caused by the difficulties in filling the dewars with sufficient amounts of liquid nitrogen, rendered data from some of the spectrographs unusable. Likewise, the 2D pipeline used to reduce the data is far from perfect and leads to many artifacts resulting from, e.g. poor sky subtraction. However, the data are nonetheless useful. In addition, characterizing and understanding the systematics that may affect the instrument's performance and data reduction are important aspects of the commissioning process. Fortunately, quasars are easily identified given their characteristic broad emission line spectra. We visually examined the 1D spectra of quasar candidates one by one, and this led to the discovery of 14 new low-redshift background quasars in the vicinity of M 31.

All of the 14 quasars were detected with reasonable signal to noise ratios. At least two emission lines were identified, allowing reliable redshift estimates (Fig. 2). In Table 1, we present properties of these newly discovered quasars, including target names (in the format of J*hhmmss.ss+ddmmss.s*), coordinates, SDSS u, g, r, i, and z magnitudes *before* extinction corrections, i-band extinctions from Schlegel et al. (1998), GSJT observation dates and spectral fiber IDs (in the format of ii-jj-kk where ii is the spectrograph number, jj the clip number and kk the fiber number), and redshifts. For quasars detected in both 2009 October and December, only observations with better data quality are listed. Spectra of the 14 quasars are presented in Figure 2. Spectra from the two consecutive exposures, each

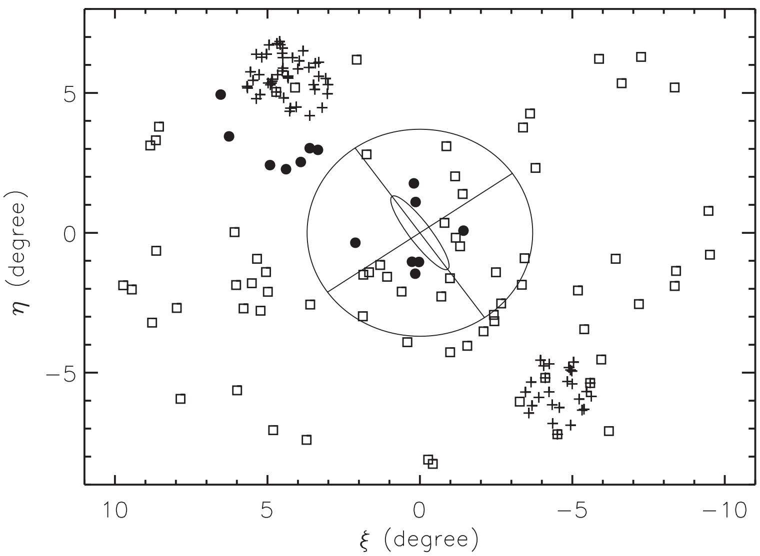

Fig. 3 Spatial distribution of background quasars in the vicinity of M 31. Filled circles, crosses and open squares represent, respectively, quasars newly identified with the GSJT, SDSS quasars, and previously known quasars archived in the NED. The inner ellipse represents the optical disk of M 31 of radius $R_{25} = 95.3'$, while the outer ellipse is a projected circle with a 50 kpc radius.

of 30 min, were coadded. Since the GSJT spectra were grossly oversampled – even at $R \sim 2\,000$, the spectral FWHM corresponds to approximately 5 pixels, so we binned the spectra by a factor of 3 to improve the signal to noise ratios. Any remaining cosmic rays were removed manually for clarity. Note that due to uncertainties in sky subtraction, some of the data points have negative values. We have made no attempt to artificially adjust the flux levels. All the newly discovered quasars have redshifts lower than 2, and are reasonably bright with i magnitudes between 16.7 and 19.2. They fall into two groups, one with redshifts around 0.4 and the other with redshifts near 1.7. This was purely due to the selection effects. For redshifts below 0.5, Hα, Hβ and the [O III] $\lambda\lambda$4959,5007 forbidden lines fall within the GSJT optical wavelength coverage, whereas for redshifts between 1.5 and 2.0, lines such as Mg II λ2800, C III] λ1908 or even C IV λ1549 are shifted into the optical wavelength range. Following the initial GSJT discoveries, we have also obtained followup observations with the Xinglong 2.16 m telescope. Quasars J010954.54+432948.3 and J010123.58+440838.4 were observed with the BFOSC (BAO Faint Object Spectrograph and Camera) on 2010 February 5. The obtained spectra confirm their quasar identifications and redshifts.

Two of the newly discovered quasars have X-ray counterparts. Within the positional uncertainties of the 20″ radius of the ROSAT all-sky survey (Voges et al. 1999), J004253.83+401334.5 and J004329.58+422209.1 coincide respectively to positions with the X-ray sources RX J0042.8+4013 and RX J0043.4+4222 detected in the first and second ROSAT PSPC surveys of M 31 (Supper et al. 1997, 2001). In addition to the 14 confirmed quasars, another 15 ‘probable’ quasars have been identified in the current GSJT dataset with either marginal signal to noise ratios or with only one emission line detected and which consequently have uncertain redshifts. Further observations are needed to clarify their identifications. Figure 3 plots the spatial distribution in the ξ–η plane of all known background quasars found in the vicinity of M 31, including 14 newly identified with GSJT, 75 SDSS quasars and 72 previously known quasars with redshifts reported in the NED archive. Here ξ and η are, respectively, RA and Dec. offsets relative to the optical center of M 31 (Huchra et al.

1991). In Figure 3, the inner ellipse represents the optical disk of M 31, assuming an optical radius $R_{25} = 95.3'$ (de Vaucouleurs et al. 1991), an inclination angle $i = 77^\circ$ and a position angle PA = 35° (Walterbos & Kennicutt 1987). The extent of the M 31 halo is quite uncertain, and a projected circle with a 50 kpc radius is shown for illustration purposes only. A distance of 785 kpc to M 31 is adopted (McConnachie et al. 2005; 1° = 13.7 kpc). Of the 14 new quasars, half of them fall within 2.5° of the M 31 center in field F03, and the other half in field F02, more than 4° from the center.

Recent large scale surveys in both optical and radio have revealed complex structures in the outer halo of M 31 extending to hundreds of kpc, pointing to M 31's violet past. A new deep 21 cm survey by Chemin et al. (2009) shows that while the regular H I disk size is approximately 27 kpc in radius, it extends out to a maximum radius of $R = 36.4$ kpc. The survey also reveals remarkable new features including an external arm which is 32 kpc long and thin H I spurs in the disk's outskirts. Thilker et al. (2004) discovered an extensive discrete H I cloud population extending out to 50 kpc. In the optical, deep imaging surveys reveal large amounts of stars and coherent structures that are almost certainly remnants of dwarf galaxies destroyed by the tidal field of M 31, as well as substructures extending all the way to the Triangulum Galaxy M 33, nearly 15° southeast of M 31 (Ibata et al. 2007; McConnachie et al. 2009), suggesting a possible recent close encounter of the two galaxies. Detailed spectroscopic analyses of the dynamics and chemistry of those relics and substructures are of paramount importance for understanding the history of M 31. However, at the distance of M 31, even red giant branch (RGB) stars have i magnitudes fainter than 20, so spectroscopic determinations of their radial velocities and chemical compositions are not easy tasks, even for a 10 m class telescope (Ibata et al. 2005; Gilbert et al. 2009). Absorption line spectroscopy of background low-redshift quasars thus provides an attractive complementary tool to probe the structure, dynamics and chemistry of baryonic matter in the vast outer region of M 31. Our current preliminary results have doubled the number of known quasars within 2.5° of M 31. At the detection limit of $i_{\rm psf} = 19.1$, we expect a surface number density of low-redshift quasars of approximately 13 deg $^{-2}$ (Richards et al. 2002). As the performance of GSJT continues to improve while the commissioning process progresses, we plan to survey the whole area of the SDSS M 31 stripes to search for low-redshift quasars, and we expect to find several hundred new background quasars. This will provide an invaluable asset to probe the environments surrounding M 31 via deep high resolution spectroscopy, especially in the UV with, e.g. the Cosmic Origins Spectrograph onboard the Hubble Space Telescope, or with future space missions such as the WSO-UV (Shustov et al. 2009).

Acknowledgements The Guoshoujing Telescope (GSJT) is a National Major Scientific Project built by the Chinese Academy of Sciences. Funding for the project has been provided by the National Development and Reform Commission. The GSJT is operated and managed by the National Astronomical Observatories, Chinese Academy of Sciences. This work has made use of the Sloan Digital Sky Survey (SDSS), the NASA/IPAC Extragalactic Database (NED) and the SIMBAD database.

References

Adelman-McCarthy, J. K., et al. 2006, ApJS, 162, 38
Adelman-McCarthy, J. K., et al. 2007, ApJS, 172, 634
Anguita, C., Loyola, P., & Pedreros, M. H. 2000, AJ, 120, 845
Bowen, D. V., Blades, J. C., & Pettini, M. 1995, ApJ, 448, 634
Boyle, B. J., Shanks, T., Croom, S. M., Smith, R. J., Miller, L., Loaring, N., & Heymans, C. 2000, MNRAS, 317, 1014
Chemin, L., Carignan, C., & Foster, T. 2009, ApJ, 705, 1395
Corbett, E. A., et al. 2003, MNRAS, 343, 705
Crampton, D., Gussie, G., Cowley, A. P., & Schmidtke, P. C. 1997, AJ, 114, 2353

Cui, X., et al. 2004, Proc. SPIE, 5489, 974
de Vaucouleurs, G., de Vaucouleurs, A., Corwin, H. G., Jr., Buta, R. J., Paturel, G., & Fouqué, P. 1991, Third Reference Catalogue of Bright Galaxies (New York: Springer)
Dobrzycki, A., Groot, P. J., Macri, L. M., & Stanek, K. Z. 2002, ApJ, 569, L15
Dobrzycki, A., Macri, L. M., Stanek, K. Z., & Groot, P. J. 2003, AJ, 125, 1330
Gebhardt, K., et al. 2000, ApJ, 539, L13
Geha, M., et al. 2003, AJ, 125, 1
Gilbert, K. M., Guhathakurta, P., Kollipara, P., Beaton, R. L., Geha, M. C., Kalirai, J. S., Kirby, E. N., Majewski, S. R., & Patterson, R. J. 2009, ApJ, 705, 1275
Haiman, Z., & Loeb, A. 1999, ApJ, 519, 479
Huchra, J. P., Brodie, J. P., & Kent, S. M. 1991, ApJ, 370, 495
Ibata, R., Chapman, S., Ferguson, A. M. N., Lewis, G. F., Irwin, M. J., & Tanvir, N. 2005, ApJ, 634, 287
Ibata, R., Martin, N. F., Irwin, M. J., Chapman, S., Ferguson, A. M. N., Lewis, G. F., & McConnachie, A. W. 2007, ApJ, 671, 1591
Luo, A.-L., Zhang, Y.-X., & Zhao, Y.-H. 2004, Proc. SPIE, 5496, 756
McConnachie, A. W., Irwin, M. J., Ferguson, A. M. N., Ibata, R. A., Lewis, G. F., & Tanvir, N. 2005, MNRAS, 356, 979
McConnachie, A. W., Irwin, M. J., Ibata, R. J., et al. 2009, Nature, 461, 66
Monk, A. S., Penston, M. V., Pettini, M., & Blades, J. C. 1986, MNRAS, 222, 787
Monk, A. S., Penston, M. V., Pettini, M., & Blades, J. C. 1988, MNRAS, 234, 193
Murdoch, H. S., Hunstead, R. W., Pettini, M., & Blades, J. C. 1986, ApJ, 309, 19
Pocock, A. S., Penston, M. V., Pettini, M., & Blades, J. C. 1984, MNRAS, 210, 373
Richards, G. T., et al. 2002, AJ, 123, 2945
Schlegel, D. J., Finkbeiner, D. P., & Davis, M. 1998, ApJ, 500, 525
Shustov, B., Sachkov, M., Gómez de Castro, A. I., Huang, M. H., Werner, K., Kappelmann, N., & Pagano, I. 2009, Ap&SS, 320, 187
Skrutskie, M. F., et al. 2006, AJ, 131, 1163
Su, D. Q., Cui, X., Wang, Y., & Yao, Z. 1998, Proc. SPIE, 3352, 76
Supper, R., Hasinger, G., Pietsch, W., Truemper, J., Jain, A., Magnier, E. A., Lewin, W. H. G., & van Paradijs, J. 1997, A&A, 317, 328
Supper, R., Hasinger, G., Lewin, W. H. G., Magnier, E. A., van Paradijs, J., Pietsch, W., Read, A. M., & Trümper, J. 2001, A&A, 373, 63
Thilker, D. A., Braun, R., Walterbos, R. A. M., Corbelli, E., Lockman, F. J., Murphy, E., & Maddalena, R. 2004, ApJ, 601, L39
Tinney, C. G. 1999, MNRAS, 303, 565
Tinney, C. G., Da Costa, G. S., & Zinnecker, H. 1997, MNRAS, 285, 111
Voges, W., et al. 1999, A&A, 349, 389
Walterbos, R. A. M., & Kennicutt, R. C., Jr. 1987, A&AS, 69, 311
Wang, S.-G., Su, D.-Q., Chu, Y.-Q., Cui, X., & Wang, Y.-N. 1996, Appl. Opt., 35, 5155
Xing, X., Zhai, C., Du, H., Li, W., Hu, H., Wang, R., & Shi, D. 1998, Proc. SPIE, 3352, 839
York, D. G., et al. 2000, AJ, 120, 1579
Zhao, Y. 2000, Proc. SPIE, 4010, 290
Zhu, Y., Hu, Z., Zhang, Q., Wang, L., & Wang, J. 2006, Proc. SPIE, 6269, 20